Effect of Periodic Blowing on Attached and Separated Supersonic Turbulent Boundary Layers

Michael S. Selig* and Alexander J. Smits†
Princeton University, Princeton, New Jersey 08544

Periodic blowing at frequencies up to 5 kHz was used to control the unsteadiness of two-dimensional shock-wave/turbulent boundary-layer interactions. Two separate experiments were performed. In the first case, periodic blowing was introduced through a spanwise slot in the wall to produce an unsteady shock-wave/boundary-layer interaction boundary layer on the tunnel wall. In the second case, periodic blowing was introduced into the shock-induced separation bubble formed by a 24-deg compression corner interaction. The incoming flow conditions for both experiments were $M_\infty = 2.84$, $Re_\infty/l = 6.5 \times 10^7$/m, and $\delta_o = 26$ mm. Measurements of the fluctuating mass flux and wall pressure were made, and the unsteady flowfield was visualized through stroboscopic schlieren videography. The measurements were conditionally sampled based on the phase of the blowing cycle. The results suggest that (at least in this case) the naturally unsteady shock motion in the compression ramp interaction does not contribute significantly to the turbulence amplification, as had been previously thought. Instead, there is strong evidence to suggest that large-scale motions associated with the maxima in the angular momentum profiles in the downstream boundary layer are responsible for the large mixing observed.

I. Introduction

THE characteristic unsteadiness of shock-wave/boundary-layer interactions was first documented by Kistler[1] in a study of a supersonic separated flow produced by a forward-facing step. It has since been observed in attached and separated compression corner flows,[2,3] blunt fin interactions,[4-6] and oblique shock interactions produced by a sharp fin at different angles of attack.[7,8] Despite this extensive experimental work, the effects of the unsteadiness on the boundary layer, and the mechanisms that cause the unsteadiness, are not well understood. The turbulence levels typically display a large amplification downstream of the shock, and shock unsteadiness has been suggested as an important mechanism for transferring mean flow energy into the turbulence.[9,10] It seems reasonable to suppose that the instantaneous shock position is affected by the incoming boundary-layer turbulence, and Debieve and Lacharme[11] confirmed that free-stream turbulence can cause the deformation and oscillation of an oblique shock. Furthermore, when the flow is separated, large-scale "breathing" of the separated zone may induce an unsteady shock motion,[9] and since the frequency of the shock motion in a compression ramp interaction depends on the ramp angle,[6] the unsteadiness may also depend on the shock strength.

The present investigation was initiated to help improve our understanding of these unsteady flows, with the specific aim of determining the effect of the unsteady shock movement on the boundary-layer turbulence. Two separate experiments were performed. In the first case, periodic blowing through a spanwise slot was used to produce an unsteady shock-wave/boundary-layer interaction on the tunnel wall at a controlled frequency. In the second case, periodic blowing was introduced near the foot of the naturally unsteady shock wave that occurs in a shock-wave/boundary-layer interaction produced by a 24-deg compression ramp placed on the tunnel wall. This particular 24-deg ramp interaction (without blowing) has been widely studied in the past.[2,12-15] It displays a large separated region (see Fig. 1), and the frequency of the "natural" shock motion varies over a wide range, with a mean below 2 kHz but with oscillations extending up to 10 kHz. The periodic blowing could be varied up to 5 kHz, and it was used to "lock in" the unsteadiness at a fixed frequency typical of the unforced shock oscillation. Since it was periodic, phase averaging could be used to identify the downstream effect of the shock oscillation. The incoming boundary layer was identical in the two experiments, and the upstream freestream Mach number was 2.84.

The apparatus used to produce the periodic blowing and details of the experimental techniques are described in Sec. II. The results, given in Secs. III and IV, indicate that the unsteadiness has only a minor effect on the flat-plate boundary layer but a strong effect on the compression ramp flow. Relatively small levels of blowing were very effective in controlling the frequency of the unsteadiness, and in changing the scale of the interaction. Despite these changes, the overall amplification of the turbulence levels was virtually unaffected. Hence, it seems that the enhanced turbulent mixing observed in the compression ramp flow is not caused by the "pumping" effect of the shock motion, contrary to previous thinking.

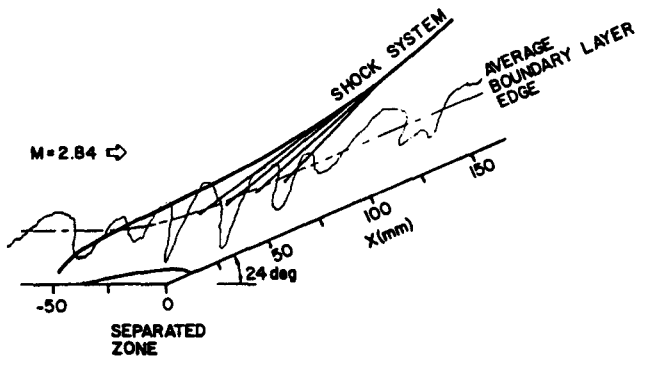

Fig. 1 Mach 2.84, 24-deg compression corner mean flowfield.

Received Jan. 22, 1990; revision received Jan. 2, 1991; accepted for publication Jan. 2, 1991.

*Graduate Student; currently at Department of Mechanical Engineering, Pennsylvania State University, University Park, PA 16802. Student Member AIAA.

†Professor, Department of Mechanical and Aerospace Engineering. Member AIAA.

Table 1 Boundary-layer characteristics and incoming flow conditions

Test conditions
p_o = 0.69 × 10^6 Pa (100 psi)
T_o = 270 K
M_∞ = 2.84
Re_∞/l = 6.5 × 10^7/m
δ_o = 26 mm
δ^* = 6.4 mm
θ_o = 1.3 mm
C_{fo} = 0.00115

Instead, it may be caused by the production of large-scale motions associated with the maxima in the angular momentum profiles downstream of the interaction.

II. Experimental Facility, Apparatus, and Test Conditions

The experiments were performed in the Princeton University 203 × 203 mm (8 × 8 in.), Mach 3, blowdown wind tunnel. For the flat-plate boundary-layer experiment, the nozzle-wall boundary layer was used. At the position of the injection slot, 1.95 m downstream of the throat, the layer was typical of a zero-pressure gradient fully turbulent boundary layer, and it obeyed both the law of the wall and law of the wake.[16,17] Its characteristics are summarized in Table 1.

For the shock-wave/boundary-layer interaction experiment, a 24-deg compression corner model was mounted on the tunnel floor downstream of the injection slot. The model was 152.4 mm wide, which left room between the model and the tunnel walls for the sidewall boundary layers to pass without interference. The model width and geometry was the same as that used by Settles,[12] Murphy,[18] and Or.[19] To improve the two-dimensionality of the flow, aerodynamic fences made of clear 6.4-mm-thick Plexiglas were screwed to the sides of the model. The edges of the fences were beveled at 30 deg to reduce aerodynamic disturbances caused by their presence.

The periodic blowing apparatus operates somewhat like a siren in that a stream of air is clipped periodically to produce a high-frequency, pulsed jet of air issuing through a spanwise slot in the floor of the test section (see Fig. 2). The slot is opened and closed by a hollow slotted drum, spinning within a pressurized plenum chamber. The frequency of the blowing

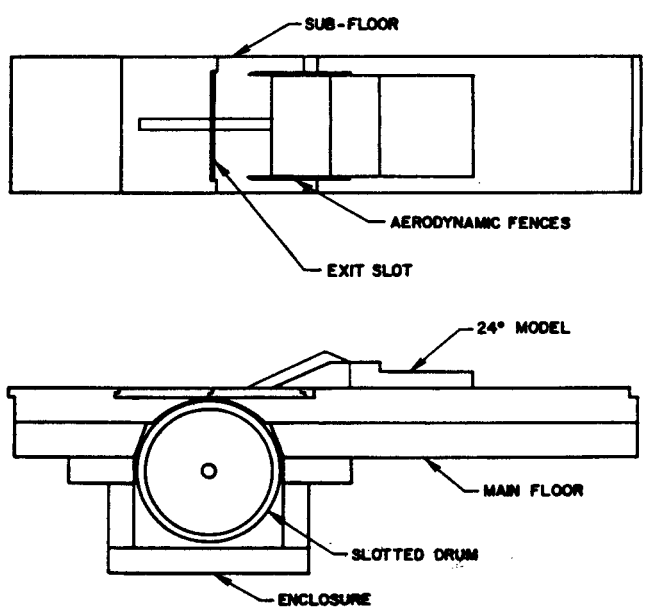

Fig. 2 Periodic blowing apparatus.

was controlled by the speed of the drum and could be safely set as high as 5 kHz. The amount of air injected through the injection slot into the boundary layer was controlled by varying the supply pressure in the plenum chamber and by varying the width of the slot. Since the flow mostly responded to the net amount of blowing rather than how it was achieved, the slot width was fixed at 3.2 mm (1/8 in.), and only the plenum chamber pressure was varied to control the blowing flow rate.

The freestream Mach number was fixed by the nozzle geometry at 2.84 ± 1%, and the stagnation pressure was held fixed at 0.69 × 10^6 Pa ± 1% (100 psia). The stagnation temperature remained fairly constant over the test period at 270 K ± 2%. The freestream turbulence level was about 1–1.5%.[20]

The static pressure variations were measured using miniature differential pressure transducers manufactured by Kulite Semiconductor Inc., Model XCQ-062-25-D. They were

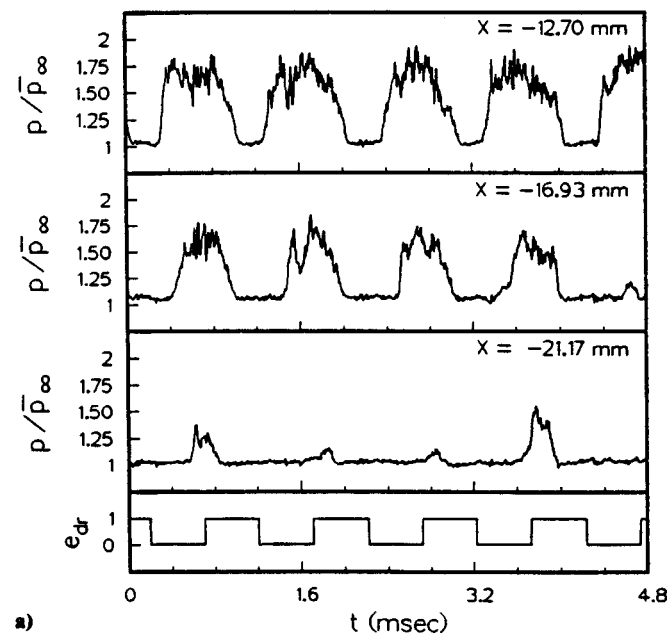

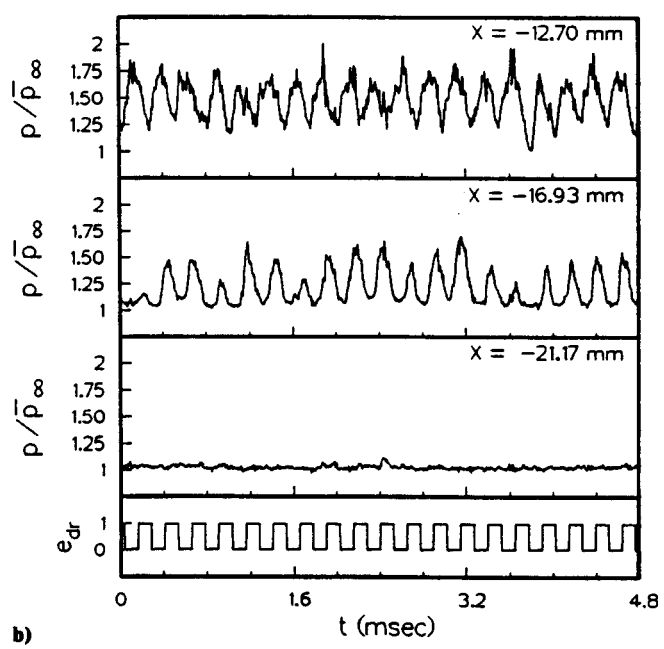

Fig. 3 Wall-pressure time histories for flat-plate boundary-layer experiment. Blowing frequency: a) 1 kHz; and b) 4 kHz. The signal marked e_{dr} indicates the blowing rate: the blowing is on when the signal is high.

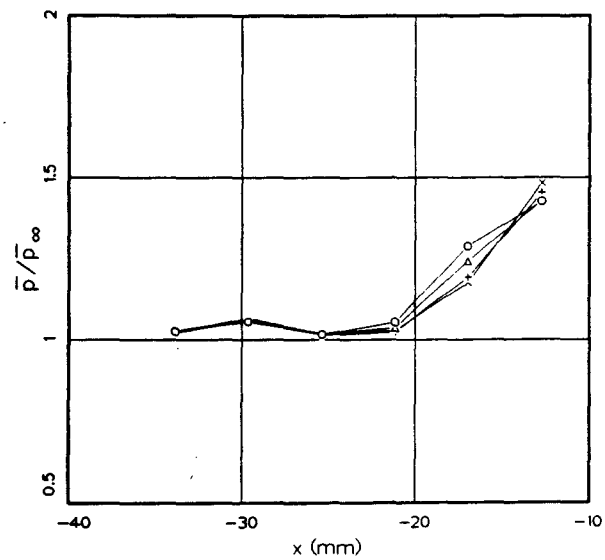

Fig. 4 Mean wall-pressure distributions for flat-plate boundary-layer experiment. Blowing frequency: ○, 1 kHz; △, 2 kHz; +, 3 kHz; and ×, 4 kHz.

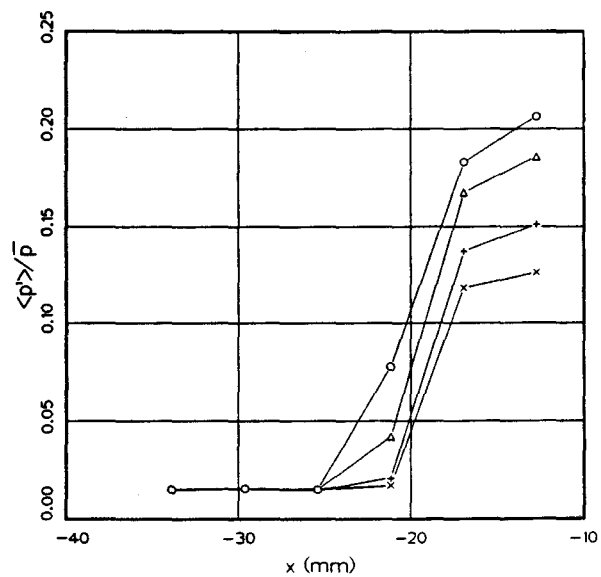

Fig. 5 Rms wall-pressure distributions for flat-plate boundary-layer experiment. Blowing frequency: ○, 1 kHz; △, 2 kHz; +, 3 kHz; and ×, 4 kHz.

calibrated statically against a known reference pressure over the range encountered in the experiment. In this study, the transducers were used primarily to reveal the dynamic character of the low-frequency shock motion (500 Hz–10 kHz) and the limited frequency response of the pressure transducers (≤ 50 kHz) was of no great concern. The transducers were positioned along the centerline of the tunnel floor, with a minimum spacing of 4.2 mm. No wall-pressure measurements were made downstream of the slot.

The fluctuations in the boundary-layer mass flux were measured using a DISA 55M10 constant-temperature hot-wire anemometer, according to the technique described by Smits et al.[21] To reduce the temperature sensitivity of the anemometer, so that the output was sensitive only to variations in mass flux, the probe was operated at an overheat ratio of 0.8, yielding an uncertainty in the measured $\langle (\rho u)' \rangle / (\rho U)$ of −5 to 9%.[22] The frequency response was always in excess of 100 kHz.

In digitizing, the anemometer and pressure transducer output signals were split into two components, a fluctuating and a mean. The mean was obtained by low-passing the signal at 10 Hz and sampling at a relatively low rate. The fluctuating part of the signal was obtained by high-passing the signal at 10 Hz. This fluctuating signal was amplified to fill the range of the A/D converter, filtered at a cutoff point of 250 kHz (anemometer), or 125 kHz (pressure transducers), then sampled at 500 kHz or 1 MHz (anemometer), or 500 kHz (pressure transducers). The signal from the drum encoder was also recorded so that the data could be phase-averaged using the blowing-cycle phase.

Every run was visualized using a schlieren videography system. The spark source of the schlieren system was strobed slightly out of phase with the periodic blowing frequency to reveal the flow response in stroboscopic "slow motion." In this way, the conventional video camera was converted into a pseudo-high-speed camera to provide "movies" of the flow. See Selig[23] and Selig et al.[15] for further details of the experimental procedure.

III. Flat-Plate Boundary-Layer Results

With the amount of blowing fixed at 9% of the freestream mass flux, that is, $(\rho V)_{slot}/(\rho U)_\infty = 0.09$, the flow was examined for blowing frequencies of 1, 2, 3, and 4 kHz. Wall-pressure data were taken upstream of the slot for each case, and mass-flux data were taken downstream for the 2-kHz case only.

Flow visualization using the schlieren videography system demonstrated that the flow structure depends on the fre-

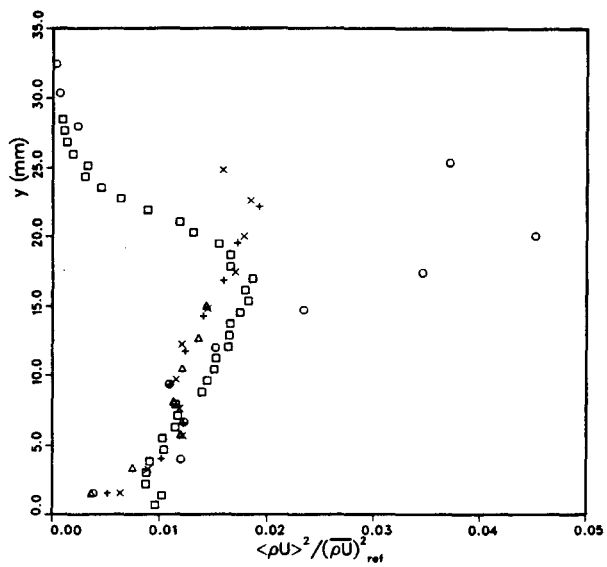

Fig. 6 Mass-flux turbulence intensity profiles for flat-plate boundary-layer experiment, 9% blowing at 2 kHz. ○, x = 12.7 mm; △, x = 25.4 mm; +, x = 38.1 mm; and ×, x = 50.8 mm.

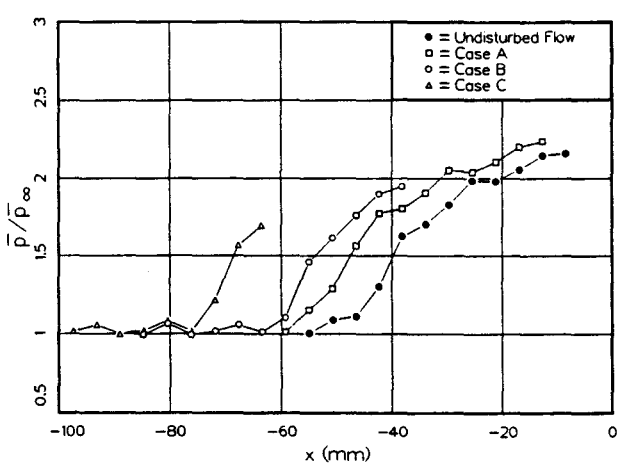

Fig. 7 Mean wall-pressure distributions for compression corner experiment: ●, no blowing; □, case A; ○, case B; and △, case C.

Table 2 Cases studied for the 24-deg compression corner with periodic blowing

Case	f_{dr}, kHz	r, %	x_s, mm
A	2	9	0
B	2	9	25.4
C	2	9	50.8
D	1	9	25.4
E	2	≤2.5	25.4
F	1	≤2.5	25.4
H	Variable	≤2.5	0

quency of blowing. At low frequencies, an oblique shock forms as the incoming flow is deflected by the blowing. As the blowing continues, this shock travels upstream at a speed of the order of 50 m/s (as measured from the time delay on adjacent pressure transducers) to reach a maximum position upstream of the slot. When the blowing stops, the shock dissipates as it is convected downstream at a speed of the order of 120 m/s. The sequence is repeated with the start of the next blowing cycle. As the blowing frequency increases, a critical frequency is reached (between 2 and 3 kHz) at which the downstream-moving shock just reaches the slot as a new blowing cycle begins. At still higher frequencies, the shock does not reach the slot before the new blowing cycle starts. As a result, the blowing triggers the formation of a second shock which itself travels upstream and intersects the first shock. The two shocks merge into one, move upstream to a maximum position, and on returning downstream encounter another shock produced by the next blowing cycle, and so on.

Wall-pressure time histories for the 1- and 4-kHz cases are shown in Fig. 3. At the lower frequency, a relatively steep rise in the mean wall pressure is seen with the passage of the shock upstream, followed by a more gradual reduction of the wall pressure as the shock passes back downstream. Behind the shock at $x = -12.7$ mm (x is measured positive downstream from the back edge of the slot), the normalized pressure rise for this 1-kHz case is roughly 1.75, which at this Mach number corresponds to an 8 deg turning of the flow with a shock angle of 27 deg. This estimated shock angle is in good agreement with that measured from the flow visualization. At the higher frequency, the pressure at $x = -12.7$ mm never returns to its upstream value, indicating that a shock wave is always located upstream of that point.

The mean wall-pressure data, given in Fig. 4, shows that the mean pressure distribution is virtually independent of the blowing frequency (the agreement is within the uncertainty of the data, which is of the order of ±10%). The rms wall-pressure levels (Fig. 5) begin to rise further downstream as the blowing frequency increases; at lower frequencies there is more time for the shock to penetrate upstream before the blowing stops. As the blowing frequency increases, the blowing period approaches the time constant of the shock motion, and as a result the maximum fluctuation level decreases at higher frequencies.

The mass-flux turbulence intensity profiles for the 2-kHz case are given in Fig. 6. The peak in the turbulence intensity profile at $x = 12.7$ mm is in the region of the shock oscillation and should not be considered as "true" turbulence. Discounting this shock-induced peak, the turbulence intensities in the outer part of the boundary level downstream of the slot are very similar to the upstream levels, except for an outward displacement of about 5 mm, probably due to the intermittent presence of the thin separated zone near the wall.

The mass-flux spectra (see Selig[23]) display a spike at the blowing frequency throughout the boundary layer, indicating that the periodic motion of the shock makes a small contribution to the turbulence. The phase-averaged results indicated that for stations downstream of $x = 12.7$ mm the periodic component contributes less than 25% to the mean square intensity.

IV. Compression Ramp Results

For the compression ramp experiment, only two blowing frequencies, 1 and 2 kHz, were used, and the slot was positioned at $x = 0$, 25.4, or 50.8 mm, where x is now measured from the corner, and x is positive in the downstream direction. The blowing level was set at either 9 or 2.5% of the freestream mass flux, and the slot width was kept constant at 3.2 mm. The combinations that were tested are listed in Table 2, where each case is identified by a letter code. For cases A/B/C only the slot position was changed, for B/D and E/F the frequency was changed, and for B/E and D/F the amount of blowing was changed. For case H only the frequency was varied.

A. Two-Dimensionality of the Flow

Surface flow patterns by the kerosene and lampblack method provide some indication of the mean separation and reattachment points. It can also be used to give an indication of the degree of two-dimensionality. The surface flow patterns obtained by Settles,[12] Murphy,[18] and Or[19] were compared with the surface flow patterns obtained during this investigation (without blowing). The traces were taken in the same tunnel.

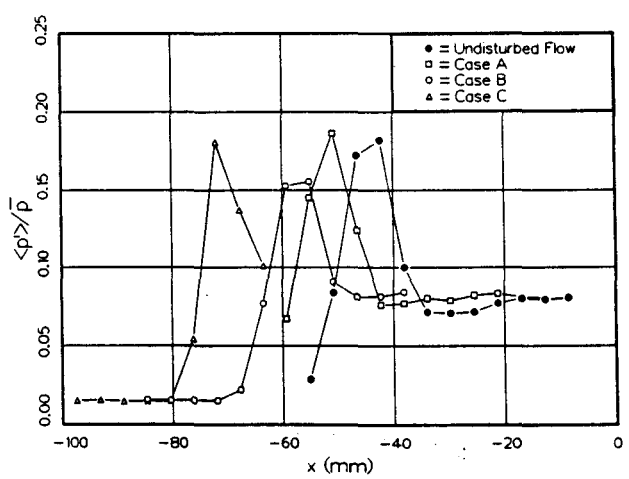

Fig. 8 Rms wall-pressure distributions for compression corner experiment. Symbols are as in Fig. 7.

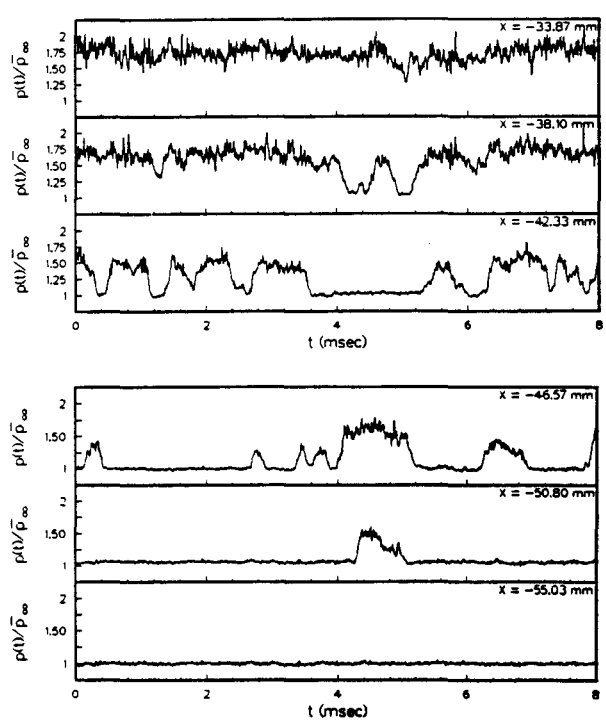

Fig. 9 Six wall-pressure time histories upstream of the compression corner (no blowing) (groups of three are simultaneous).

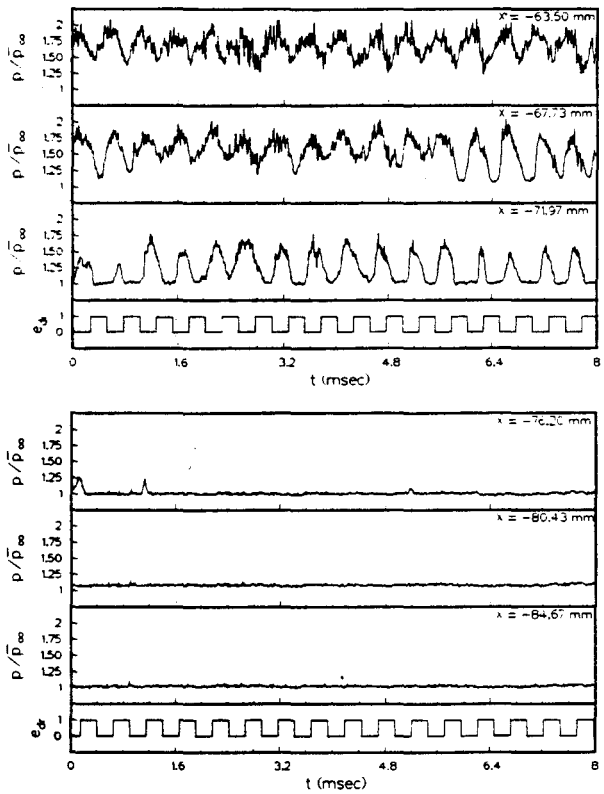

Fig. 10 Six wall-pressure time histories upstream of the compression corner for case C (groups of three are simultaneous). The signal marked e_{dr} indicates the blowing rate: the blowing is on when the signal is high.

under nominally the same conditions, and with the same 24-deg compression corner geometry. Some features were observed in all cases. For example, the mean separation line (as indicated by the surface flow visualization) was located at an average position of about 34 mm upstream of the corner, with a waviness amplitude of 2–6 mm. The waviness itself, however, sometimes displayed a regular cellular pattern, and in other cases it was rather irregular. Smits and Muck[10] suggested that the waviness may indicate the presence of longitudinal roll cells produced by a Taylor-Gortler-like mechanism. It could be that, with time, the accumulation of dirt on the screens in the settling chamber caused the roll cells to originate at different spanwise locations. Despite these differences, it is clear that all of the experiments on this compression ramp indicate that three-dimensional effects are an integral part of this nominally two-dimensional flow.

B. Wall-Pressure Distributions

The mean and fluctuating wall-pressure distributions, are shown in Figs. 7 and 8. The agreement with the earlier measurements in the same flow[2,3,17] (without blowing) is within experimental error, that is, ±10% on the mean, and ±20% on the rms (see also Selig et al.[15] Figs. 3 and 4).

Periodic blowing can strongly influence the wall-pressure distributions; the results given in Fig. 7 show that as the slot is moved upstream, the point where the wall pressure first rises moves upstream as well, with little change in the shape of the distribution. The corresponding rms wall-pressure results given in Fig. 8 show the same forward shift with little change in the region near the peak in the rms level. The wall-pressure time histories (Figs. 9 and 10) indicate that as the slot is moved upstream, the shock begins to oscillate at the frequency of the blowing, moving upstream at about 70 m/s, and downstream at about 120 m/s. When the slot is located at $x = -51$ mm, the shock is locked in, and its movement is completely controlled by the periodic blowing. As a result, the mean shock location is shifted upstream. Despite these significant changes, neither the mean wall-pressure gradient nor the rms levels in the vicinity of the shock show any appreciable change. They appear as if the entire compression corner were moved upstream rather than just the slot.

The effect of varying the amount and the frequency of blowing was found by examining cases D–H. Both the mean wall-pressure rise and the rms levels for cases B and D (2 and 1 kHz, respectively) were essentially the same, as were cases E and F for lighter blowing. The rms wall-pressure data for case H, where the frequency was varied from 1.5 to 2.5 kHz, again showed virtually no change with variation in frequency. There does not seem to be a natural frequency of oscillation, at least over the frequency range examined. As for the effect of the amount of blowing, the mean shock position moved upstream with an increase in blowing.

The energy spectra of the wall pressure fluctuations indicated that for the case of no blowing, the wall-pressure fluctuations in the region between $x = -55$ and -34 mm are clearly dominated by the broadband low-frequency oscillations of the shock. With no blowing, the shock randomly

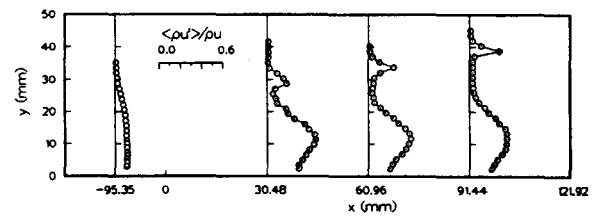

Fig. 11 Mass-flux turbulence intensity profiles in compression corner flow (no blowing).

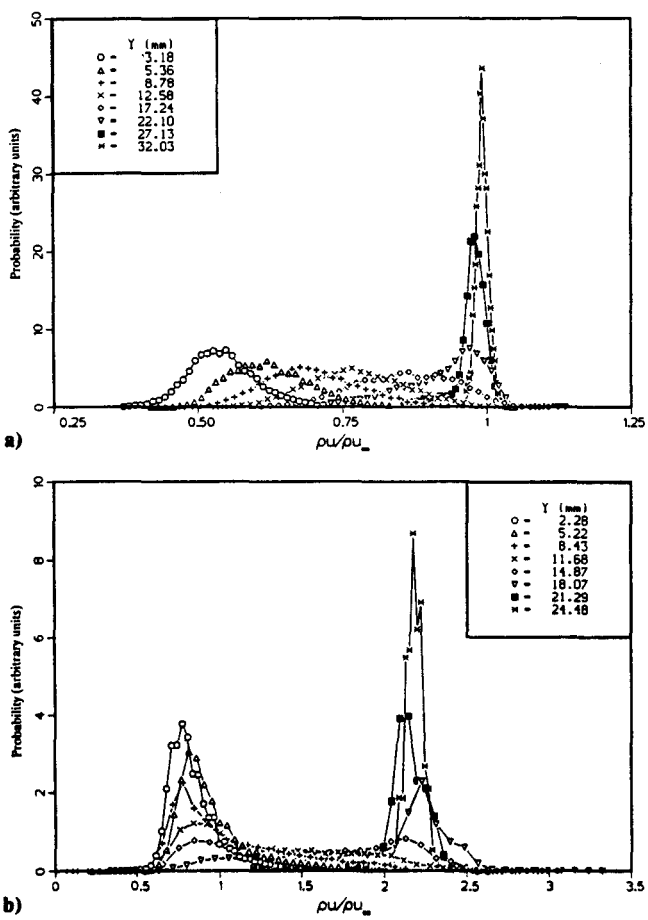

Fig. 12 Probability density functions of the mass-flux profiles in compression corner flow (no blowing): a) $x = -95.4$ mm; ○, $y = 3.2$ mm; △, 5.4; +, 8.8; ×, 12.6; ◇, 17.2; ▽, 22.1; ☒, 27.1; and *, 32.0. b) $x = 91.4$ mm; ○, $y = 2.3$ mm; △, 5.0; +, 8.2; ×, 11.4; ◇, 14.6; ▽, 17.8; ☒, 20.9; and *, 24.0.

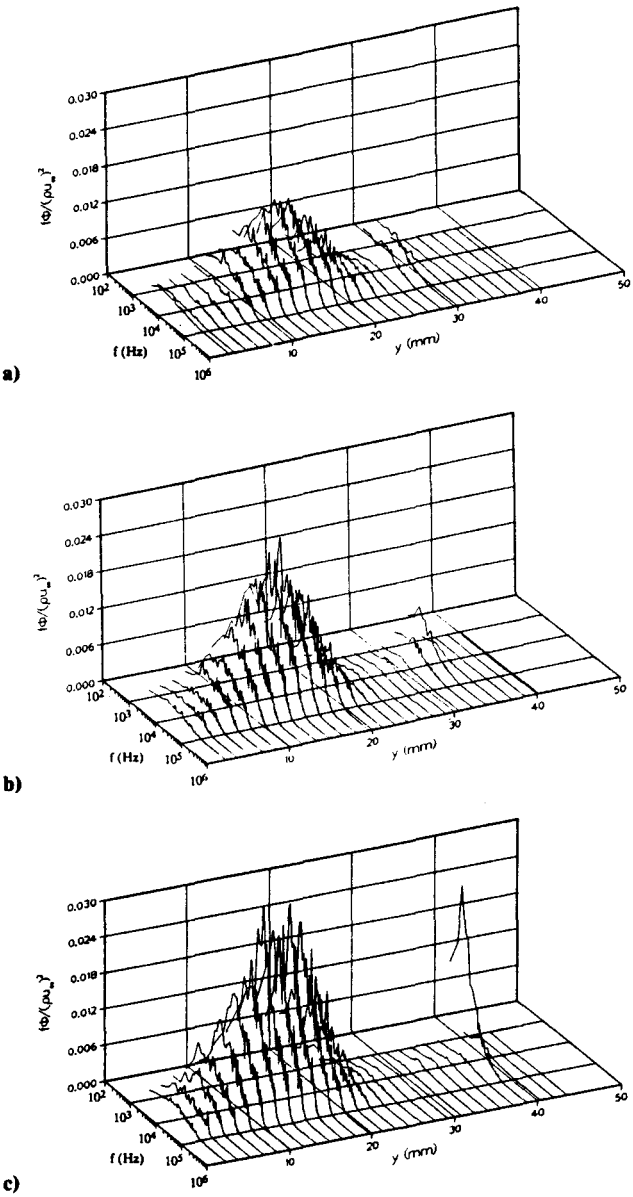

Fig. 13 Energy spectra of the mass flux in compression corner flow (no blowing): a) x = 30.5 mm; b) x = 61.0 mm; and c) x = 91.4 mm.

oscillates at a mean between 1 and 2 kHz,[2] although the distribution is highly skewed and extends up to a frequency of 10 kHz.[14] One might expect that these low-frequency shock oscillations produce low-frequency pressure fluctuations that convect downstream into the separated region. On the contrary, it was found that immediately behind the shock the low-frequency fluctuations are small compared with the high-frequency fluctuations that grow in strength towards the corner.

The spectra were also measured for the cases with blowing. For case A, spikes at the blowing frequency and its higher harmonics were present in the shock region, although the flow visualization and wall-pressure time histories gave no obvious indication of periodic shock motion. These spikes rapidly attenuated downstream but then remained at an approximately constant level in the separated zone. The high-frequency components (> 5 kHz) were not affected. For case B, the spikes in the spectra were larger, and even larger for case C as the oscillations become more regular. In all cases, there was evidence of a periodic fluctuation at the blowing frequency in the separated zone. It could not be deduced from the spectra whether this periodicity originated from upstream travelling disturbances produced by blowing, or from downstream convecting pressure fluctuations caused by the oscillating shock. The longitudinal (or streamwise) space-time correlations of the wall pressure (see Selig[2,3]) indicated that the fluctuations were convected to downstream and hence were related to the shock oscillation. The maxima in the streamwise space-time correlations of the wall pressure at the base of the shock were positive for both positive and negative time delays, corresponding to downstream and upstream movement of the shock front, respectively. The maximum correlation, however, occurred for negative time delays because the upstream movement of the shock was stronger and more coherent than the downstream movement. This was true with and without blowing, and it seems probable that the unsteadiness of the shock for the 24-deg compression corner is partially driven by large-scale fluctuations in the separated region.

C. Mass-Flux Turbulence Behavior

The rms mass-flux turbulence intensity profiles for the case with no blowing are shown in Fig. 11. Although the compression increases the freestream mass flux by a factor of 2.0, the maximum rms level in the downstream boundary layer (x = 101.6 mm, see Ref. 15) increases to 4.8 times the value found upstream of the interaction.

The probability density functions (pdfs) of the mass flux, shown in Fig. 12, indicate that the upstream pdfs have Gaussian-like distributions with a mean that gradually increases up

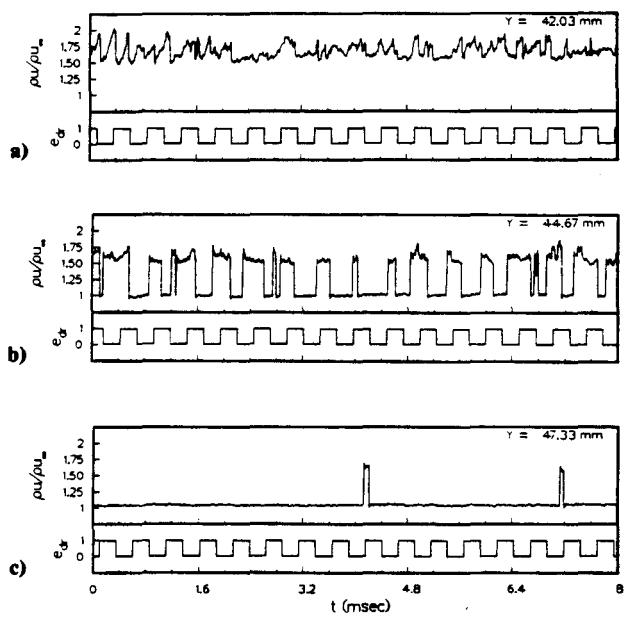

Fig. 14 Mass-flux time histories at x = 91.4 mm for compression corner flow case B: a) y = 42.0 mm; b) y = 44.7 mm; and c) y = 47.3 mm. The signal marked e_{dr} indicates the blowing rate: the blowing is on when the signal is high.

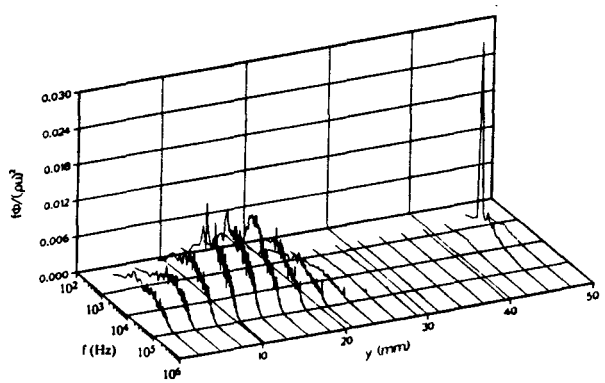

Fig. 15 Energy spectra of the mass flux for compression corner flow (case B, x = 91.4 mm).

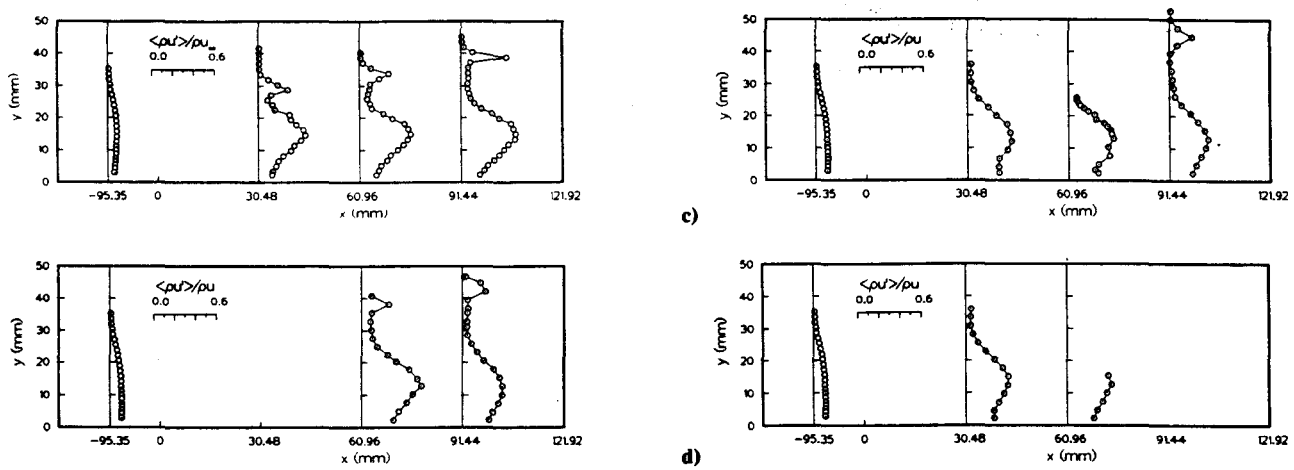

Fig. 16 Mass-flux turbulence intensity profiles for compression corner flow: a) no blowing; b) case A; c) case B; and d) case C.

through the boundary layer. In sharp contrast, the downstream pdfs center around two distinct mass-flux levels. The mass flux begins to center around $0.75\rho U_\infty$ for $y < 11.7$ mm, and around $2.2\rho U_\infty$, equal to the freestream value downstream of the interaction, for $y > 18.1$ mm. Between $y = 11.7$ and 18.1 mm, the pdfs are bimodal, and here the turbulence intensities are largest. Apparently, the mass flux fluctuates between two distinct levels, one level representative of the freestream behind the shock and another level representative of the flow very near the wall. A similar behavior was found near the reattachment point of compressible reattaching shear layer by Hayakawa et al.[24]

Energy spectra for some of the hot-wire data are given in Fig. 13. Downstream at $x = 91.4$ mm, the spectra in the freestream ($y = 40$ mm) are dominated by frequencies below 6 kHz with a maximum near 1 kHz, very much like the wall-pressure spectra near the foot of the shock. The low-frequency shock oscillations in the freestream do not appear to produce low-frequency fluctuations in the mass flux between the boundary-layer edge and the shock. A similar result was found by Debieve and Lacharme[11] in an experimental study of freestream turbulence interacting with an unsteady shock; the upstream turbulence spectra were very much like the downstream, even though in the region of the shock a large amount of low-frequency energy was found in the spectra due to shock oscillation.

Within the boundary layer, the maxima in the spectra are located near 10 kHz which is an order of magnitude higher than the mean frequency of the shock motion. In contrast, Ardonceau et al.[25] found for a separated 18-deg compression corner two broad peaks in the downstream spectra. One peak closely resembled the peak observed in the present flow—a high-frequency peak well above the unsteady shock frequency present at all points in the boundary layer. A second peak appeared near the wall (for $y < 0.56\delta_{,,}$ where $\delta_{,,} \approx 8$ mm) at a frequency characteristic of the low-frequency fluctuations of the separated region. No such low-frequency peak was observed in the present flow. Perhaps these differences are related to the flow regimes that were studied. In the present study, $Re_{,,}/l$ was 5.9 times larger, and $Re_{\delta_{,,}}$ was 17 times larger than that of Ardonceau et al.[25]

Measurements of the turbulent mass flux were also made with periodic blowing applied. Time histories of the mass flux in the vicinity of the shock outside of the boundary layer at $x = 91.4$ mm for case B are shown in Fig. 14. The flow at $y = 42.0$ mm is just beneath the shock, $y = 44.7$ mm is in the region of the shock, and $y = 47.3$ mm is nearly in the freestream ahead of the shock. From the data at $y = 44.7$ mm, it is clear that in the freestream the shock oscillates at the frequency of the blowing with some variability in phase. Flow visualization showed that the oscillations at the foot of the shock travel along the shock with a wavelength estimated to be longer than $20\delta_{,,}$ (for blowing at 2 kHz). At higher frequencies the wavelength was reduced.

The spectra with blowing (case B, $x = 91.4$ mm only) are shown in Fig. 15. At $y = 44.7$ mm (well outside the boundary layer), there is a distinct spike at 2 kHz, but for $y < 44.7$ mm there is no sign of the periodic blowing; no dominant spectral peaks are seen at the blowing frequency. Aside from slight differences, spectra with and without blowing for the same x station are essentially the same. It is therefore not surprising to find that the turbulence intensity profiles for cases A–C shown in Fig. 16 are like those seen without blowing (Fig. 11). The phase-averaged mass-flux measurements indicated that the periodic component contributed less than 2% to the mean square intensity, in contrast to the flat-plate experiment where it contributed about 25% of the mean square intensity (see Sec. III). Furthermore, the bimodal quality of the mass-flux pdf did not change from the undisturbed flow case. The shock and the separated region apparently have little impact on the turbulence amplification.

V. Conclusions

Periodic blowing was found to have relatively little effect on the flat-plate boundary layer but a strong effect on the compression ramp flow. Relatively small levels of blowing were very effective in controlling the frequency of the unsteadiness in the ramp flow, depending on the amount and location of the blowing. Increasing the amount of blowing and moving the blowing closer to the foot of the shock moved the mean position of the shock upstream and increased the degree of the forced periodicity.

The speed of the shock motion in both the upstream and downstream directions was only a fraction of the freestream velocity, and it was not strongly affected by blowing. Andreopoulos and Muck[14] in their study of compression ramp flows found that the mean frequency of the shock oscillation was constant for corner angles from 16 to 24 deg. However, since the zone of shock oscillation increases with corner angle, and the results from periodic blowing showed there were limits on the shock speed, the frequency should not be constant but vary inversely with an amplitude or the range of shock oscillation; i.e., the frequency should be higher for smaller turning angles. Indeed Dolling and Brusniak,[26] using a sophisticated conditional-sampling method, found that the mean frequency of the oscillation increased with decreasing ramp angle.

It is a widely held view that part of the turbulence amplification in shock-wave/boundary-layer interactions is caused by the unsteady shock motion. It was shown here that the direct effects of the unsteady shock motion on the turbulence were small in the flat-plate experiment, and insignificant in the separated compression ramp experiment. This result may

follow directly from the observation that the frequency band of the shock motion has only a small overlap with the frequency band of the incoming turbulence. This is true for the forced, and the unforced case, since the frequency of the shock motion was similar for both cases. For flows where this overlap is more significant, a stronger coupling is to be expected.

Instead, we suggest that the turbulence amplification in the compression ramp flow studied here is caused primarily by two mechanisms: "inviscid" amplification by compression through the interaction, and large-scale mixing processes associated with the separating and reattaching shear layer. These mixing processes may be driven by instabilities in the outer part of the boundary layer, or possibly through the presence of unsteady longitudinal Taylor-Gortler type vortices that form in the concavely curved separated shear layer. Both mechanisms can move low-speed momentum fluid up from the wall and high-speed momentum fluid down from the freestream. The shear-layer instabilities may be especially strong: Morkovin[27] has argued that generalized inflectional instabilities are centered on local maxima of mean $-\rho\, \partial U/\partial y$, the angular momentum, and such maxima were observed in the angular momentum profiles downstream of the interaction.

Acknowledgments

This work was supported by the U.S. Army Research Office, under Contract DAAG29-K-0255, monitored by T. L. Doligalski. E. Fernando's help in processing some of the conditionally sampled data is gratefully acknowledged.

References

[1]Kistler, A. L., "Fluctuating Wall Pressure Under a Separated Supersonic Flow," *Journal of the Acoustical Society of America*, Vol. 36, No. 3, 1964, pp. 543–550.

[2]Dolling, D. S., and Murphy, M. T., "Unsteadiness of the Separation Shock Wave in a Supersonic Compression Ramp Flowfield," *AIAA Journal*, Vol. 21, No. 12, 1983, pp. 1628–1634.

[3]Dolling, D. S., and Or, C. T., "Unsteadiness of the Shock Wave Structure in Attached and Separated Compression Corner Flowfields," AIAA Paper 83-1715, July 1983.

[4]Kaufman, L. G., Korkegi, R. H., and Morton, L. C., "Shock Impingement Caused by Boundary-Layer Separation Ahead of Blunt Fins," AIAA Paper 73-236, Jan. 1973.

[5]Dolling, D. S., and Bogdonoff, S. M., "Blunt Fin-Induced Shock Wave Turbulent Boundary-Layer Interaction," *AIAA Journal*, Vol. 20, No. 12, 1982, pp. 1674–1680.

[6]Dolling, D. S., "Unsteadiness of Shock Wave-Induced Turbulent Boundary-Layer Separation—A Review," *IUTAM Symposium on Turbulent Shear-Layer/Shock Wave-Interaction*, Palaiseau, France, Sept. 1985.

[7]Tan, D. K. M., Tran, T. T., and Bogdonoff, S. M., "Surface Pressure Fluctuations in a Three-Dimensional Shock-Wave/Turbulent Boundary-Layer Interaction," AIAA Paper 85-0125, Jan. 1985.

[8]Tran, T. T., Tan, D. K. M., and Bogdonoff, S. M., "Surface Pressure Fluctuations in a Three-Dimensional Shock-Wave/Turbulent Boundary-Layer Interaction at Various Shock Strengths," AIAA Paper 85-1562, July 1985.

[9]Zang, T. A., Hussaini, M. Y., and Bushnell, D. M., "Numerical Computations of Turbulence Amplification in Shock-Wave Interactions," *AIAA Journal*, Vol. 22, No. 1, 1984, pp. 13–21.

[10]Smits, A. J., and Muck, K. C., "Experimental Study of Three Shock Wave/Turbulent Boundary-Layer Interactions," *Journal of Fluid Mechanics*, Vol. 182, Sept. 1987, pp. 291–314.

[11]Debieve, J. F., and Lacharme, T. P., "A Shock-Wave/Free Turbulent Interaction," *IUTAM Symposium on Turbulent Shear-Layer/Shock-Wave Interaction*, edited by J. Delery, Springer-Verlag, Berlin, 1986, pp. 393–403.

[12]Settles, G. S., "An Experimental Study of Compressible Turbulent Boundary-Layer Separation at High Reynolds Numbers," Ph.D. Thesis, Dept. of Aerospace and Mechanical Sciences, Princeton Univ., Princeton, NJ, 1975.

[13]Settles, G. S., Fitzpatrick, T. J., and Bogdonoff, S. M., "Detailed Study of Attached and Separated Compression Corner Flowfield in High-Reynolds-Number Supersonic Flow," *AIAA Journal*, Vol. 17, No. 6, 1979, pp. 579–585.

[14]Andreopoulos, J., and Muck, K. C., "Some New Aspects of the Shock-Wave/Boundary-Layer Interaction in Compression Ramp Flows," *Journal of Fluid Mechanics*, Vol. 180, July 1987, pp. 405–428.

[15]Selig, M. S., Andreopoulos, J., Muck, K. C., Dussauge, J. P., and Smits, A. J., "Simultaneous Wall-Pressure and Mass-Flux Measurements Downstream of a Shock-Wave/Turbulent Boundary-Layer Interaction," *AIAA Journal*, Vol. 27, No. 7, 1989, pp. 862–869.

[16]Taylor, M. W., "A Supersonic Turbulent Boundary Layer on Concavely Curved Surfaces," M.Sc. Thesis, Mechanical and Aerospace Engineering Dept., Princeton Univ., Princeton, NJ, 1984.

[17]Settles, G. S., Vas, I. E., and Bogdonoff, S. M., "Incipient Separation of a Supersonic Turbulent Boundary Layer at High Reynolds Numbers," *AIAA Journal*, Vol. 14, No. 1, 1976, pp. 50–56.

[18]Murphy, M. T., "An Experimental Investigation of the Separation Shock-Wave Unsteadiness in a Compression Corner Flowfield," M.Sc. Thesis, Mechanical and Aerospace Engineering Dept., Princeton Univ., Princeton, NJ, 1983.

[19]Or, C. T., "Unsteadiness of the Shock-Wave Structure in Attached and Separated Compression Ramp Flowfields," M.Sc. Thesis, Mechanical and Aerospace Engineering Dept., Princeton Univ., Princeton, NJ, 1985.

[20]Spina, E. F., and Smits, A. J., "Organized Structures in a Compressible Turbulent Boundary Layer," *Journal of Fluid Mechanics*, Vol. 182, Sept. 1987, pp. 85–109.

[21]Smits, A. J., Hayakawa, K., and Muck, K. C., "Constant Temperature Hot-Wire Anemometer Practice in Supersonic Flows: Pt. I—The Normal Wire," *Experiments in Fluids*, Springer-Verlag, Berlin, 1983, pp. 83–92.

[22]Smits, A. J., and Dussauge, J. P., refer to Chap. 5 of Fernholz et al., AGARDograph No. 315, AGARD, Neuilly-sur-Seine, France, 1988.

[23]Selig, M. S., "Unsteadiness of Shock-Wave/Turbulent Boundary Layer with Dynamic Control," M.Sc. Thesis, Mechanical and Aerospace Engineering Dept., Princeton Univ., Princeton, NJ, 1988.

[24]Hayakawa, K., Smits, A. J., and Bogdonoff, S. M., "Turbulence Measurements in a Compressible Reattaching Shear Layer," *AIAA Journal*, Vol. 22, No. 7, 1984, pp. 889–895.

[25]Ardonceau, P. L., Lee, D. H., Roquefort, T. A., and Goethals, R., "Turbulence Behavior in a Shock-Wave/Boundary-Layer Interaction," AGARD-CP-271, 1978.

[26]Dolling, D. S., and Brusniak, L., "Separation Shock Motion in Fin, Cylinder, and Compression Ramp-Induced Turbulent Interactions," *AIAA Journal*, Vol. 27, No. 6, 1989, pp. 734–742.

[27]Morkovin, M. V., "Transition at Hypersonic Speeds," Institute for Computer Applications in Science and Engineering, Interim Rept. 1, Hampton, VA, 1988.